NRC Research Press

ARTICLE

On the problem of a vertical gas flow through an orifice with non-standard pressure tappings locations

Yana Nec and Greg Huculak

Abstract: A comprehensive model was developed to compute the flow rate in a vertical pipe collecting gas in a landfill facility. The model accounts for gravity, viscosity, adjustable orifice diameter and non-standard locations of the pressure tappings, so placed to prevent damage to certain measuring sensors caused by atomized water entrained in the gas and pooling at the orifice plate.

Key words: orifice, flow rate, discharge coefficient, Darcy-Weisbach flow.

Résumé : Un modèle global a été développé pour calculer les débits dans une conduite verticale de collecte de gaz installée sur un site d'enfouissement de déchets. Ce modèle tient compte de la gravité, de la viscosité, du diamètre ajustable de l'orifice de la conduite et du positionnement des prises manométriques. On place ces derniers de manière à éviter l'endommagement de certains capteurs de mesure causé par la condensation de vapeur d'eau sur la plaque située à l'orifice de la conduite et par l'eau atomisée entraînée par le gaz. [Traduit par la Rédaction]

Mots-clés : orifice, débits, coefficient de débit, équation de Darcy-Weisbach.

1. Flow geometry and conditions

The current contribution was inspired by an unusual flow setting in a facility collecting landfill gas via a series of vertical wells. An orifice flowmeter with an adjustable aperture measures the pressure drop within the convecting pipe of each well. Orifice plates of diameter $\frac{3}{8}'' \le d \le 1''$ can be installed according to the flow produced by the landfill, the aperture varied to improve the measurement accuracy thereof. The pressure tappings are located $2D$ upstream and downstream of the plate (D is pipe diameter), an arrangement that is unusual and unaccounted for by the calibration manual supplied with commercial flowmeters. This atypical arrangement was necessary due to water vapour condensing on the orifice plate and interfering with the measurement sensors.

In addition to the flowmeter an instrument monitoring the gas composition records the fractions of CH_4, O_2, and CO_2. The landfill also produces N_2, as well as several other gases in quantities negligible for the purport of flow rate computation. It is thus assumed that the fluid consists of CH_4, O_2, CO_2, and N_2. The flow rate in each well might vary significantly with time as the decomposition reactions within the landfill cannot be controlled.

The classic model relies on the pressure sensors located far upstream of the constriction and immediately downstream of the orifice plate. This arrangement entails modelling through Bernoulli's equation with an empirical correction. The current setting is essentially different. The narrow jet of fluid emerging from the orifice expands and mixes with the virtually stagnant fluid immediately beyond, therefore ineluctably losing momentum. The downstream sensor is placed approximately where the jet width reaches the pipe diameter (see Fig. 1), and the pressure is measured when the mixing is almost complete. This flow cannot be modelled by Bernoulli's equation. The proposed model accounts for this atypical placement of the pressure sensors and the high variation in the flow rate. Section 2 presents a succinct review of the procedure classically used in similar applications. Sections 3 and 4 describe the new model and its validation.

2. Classic orifice model

Gas flow in industrial orifice flowmeters is classically assumed isothermal and modelled by Bernoulli's principle for incompressible and inviscid fluids, amended by an empirical correction. The flow velocity is taken uniform over the cross-section. Bernoulli's principle stems directly from Navier-Stokes equations for one dimensional, inviscid and incompressible flow, reading (excluding gravity)

$$\frac{1}{2}u^2 + \frac{p}{\rho} = \text{const} \tag{1}$$

where u, p, ρ are the flow velocity, pressure and density respectively. Applying eq. (1) between the upstream section (quantities with subscript $(\cdot)_{up}$, refer to Fig. 1) and the orifice plate (quantities with subscript $(\cdot)_{orf}$) yields the theoretical volumetric flow rate

$$q_{th} = \frac{\sqrt{2}\,A_{orf}}{\sqrt{1-\beta^4}}\sqrt{\frac{p_{up}-p_{orf}}{p_{up}}\,R\,T} \tag{2}$$

where

$$\beta = d/D \tag{3}$$

is the orifice constriction ratio. Here the ideal gas state equation $p = \rho RT$ was used, T denotes temperature and R is the specific gas constant. The cross-sectional area is denoted by A. Usually β is sufficiently small for β^4 to be simply neglected.

Received 20 October 2014. Accepted 25 May 2015.

Y. Nec. Department of Mathematics, Mount Allison University, 67 York street, Sackville, NB, Canada.
G. Huculak. GNH Engineering, 20 50th street, Delta, BC, Canada.
Corresponding author: Yana Nec (e-mail: cranberryana@gmail.com).

Fig. 1. Flow geometry schematic. Stagnant regions in the proximity of the orifice are shaded in grey.

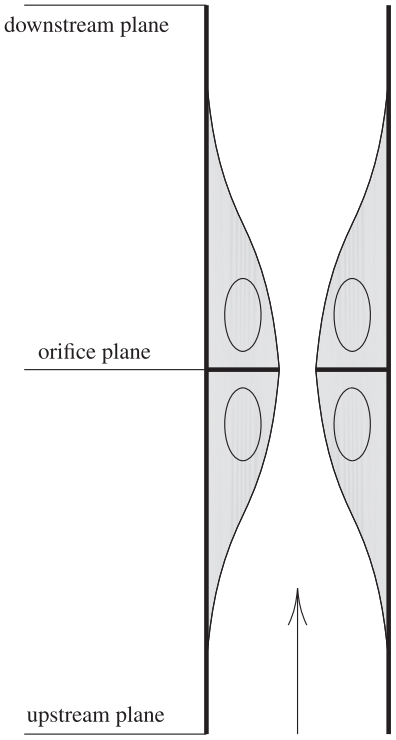

The principle of operation of standard flowmeters is based on eq. (1). The pressure is measured upstream of the orifice and immediately downstream of it, and the difference is used to compute the flow rate. Equation (1) does not account for the momentum loss due to the interaction with the stagnant regions near the orifice, non-uniformity of the velocity profile, gas compressibility and viscosity. The typical Mach number in this system does not exceed 0.05, rendering the assumption of incompressibility fairly sound, however the other phenomena require attention. To obtain a more realistic flow rate, q_{th} as given by eq. (2) is merely multiplied by a constant provided with the particular flowmeter used, usually $C \approx 0.8$:

$$q = C\, q_{th}. \tag{4}$$

The locations of the pressure tappings are prescribed in accordance with the calibration thereof. The flowmeter is calibrated for air at $T = 20$ °C and $p_{up} = 1$ atm, and thus the measured flow rate must be further corrected for the atmospheric conditions by using measured values for p and T, and for a different gas by computing R with the aid of the universal gas constant R_o, recorded gas composition fractions x_i and molar weight of the components M_i (M is mixture molar weight)

$$R = \frac{R_o}{M} = \frac{R_o}{\sum_{i=1}^{k} x_i M_i}, \tag{5}$$

where k is the number of components.

3. Current setting flow model

The classic model is inadequate for three reasons. First, with the downstream pressure sensor not placed immediately after the orifice, the mixing due to the interaction of the jet emerging from the orifice with the virtually stagnant medium beyond is overlooked. From a computational point of view this is evident from the pressure difference used in eq. (2). In the current setting it is necessary to mend eq. (2) so that the input pressure difference is that between the upstream and downstream sections. Second, when a commercial flowmeter is calibrated, the calibration constant is unique and β in eq. (2) is neglected. Here due to the high variation in the flow rate different orifice apertures are installed, when a significant change is detected. Hence the constriction ratio is not taken into account altogether except indirectly through the pressure drop created thereby. The third and often least detrimental from the aspect of precision is the assumption of horizontality in eq. (2). Taking gravity into account for a vertical flow becomes indispensable when the gas is nearly stagnant, i.e., the kinetic energy of the flow is of the same order of magnitude as the potential required to oppose the gravity field. The purpose of the proposed model is to remedy the insufficient flexibility of the classic procedure regarding the constriction ratio, whilst taking into account the effects of mixing and gravity.

3.1. Theoretical flow rate

In the classic setting the flowmeter is horizontal and thus unaffected by gravity. In the current application the vertical orientation of the well implies that for the gas to flow it must possess sufficient energy to move against the gravity field. Taking into consideration the losses due to friction with the surface of the pipe eq. (1) becomes

$$\frac{1}{2}u^2 + \frac{p}{\rho} + gh = -\frac{1}{2}u^2 c_f \frac{S}{A}, \tag{6}$$

where g is the gravity constant, h is an elevation above some reference point, c_f is the friction coefficient, and S is the surface area between the sections in question. Correspondingly eq. (2) becomes

$$q_{th} = \frac{\sqrt{2}\,A_{orf}}{\sqrt{1 - \beta^4 + 4\beta^4 c_{f_{up}} \dfrac{\ell_{up}}{D}}} \sqrt{\frac{p_{up} - p_{orf}}{p_{up}} RT - g\ell_{up}} \tag{7}$$

with ℓ_{up} being the distance between an upstream section, where the flow is uniform, and the orifice plane. The compound S_{up}/A_{up} was simplified with $S_{up} = \pi D \ell_{up}$ and $A_{up} = \frac{1}{4}\pi D^2$.

When vapour does not condense as readily on the orifice plate, pressure sensors can be installed in its proximity. The current setting necessitated an atypical placement of the tappings a distance of $2D$ up and down the stream of the orifice plane. It is therefore necessary to modify eq. (7) so that the readings can be taken at those sections. To this end expand (downstream quantities denoted by subscript $(\cdot)_{dn}$)

$$p_{up} - p_{orf} = p_{dn} - p_{orf} + p_{up} - p_{dn} \tag{8}$$

The difference $p_{up} - p_{dn}$ is to be measured and used as input in the computation of the flow rate. The difference $p_{dn} - p_{orf}$ can no longer be inferred with the aid of eq. (6) due to the mixing taking place, when the jet emerges from the orifice into the virtually quiescent gas beyond. To obtain $p_{dn} - p_{orf}$ consider the control volume between the orifice plate and downstream section. Integral momentum conservation yields (Batchelor 1990)

$$p_{dn} - p_{orf} = \rho\, u_{dn}(u_{orf} - u_{dn}) - \frac{1}{2}u^2 c_{f_{dn}} \frac{\ell_{dn}}{D} - \rho g \ell_{dn}, \tag{9}$$

where ℓ_{dn} is the distance between the downstream section and orifice plane, and a similar simplification of the compound S_{dn}/A_{dn} was made. Rearranging eq. (7) accordingly with the aid of $q_{th} = u_{orf}A_{orf} = u_{dn}A_{dn}$ (mass conservation) results in

$$q_{th} = \frac{\sqrt{2}\,A_{orf}}{\sqrt{(1-\beta^2)^2 + 4\beta^4(\alpha c_{f_{up}} + (1-\alpha)c_{f_{dn}})\frac{\ell}{D}}} \times \sqrt{\frac{p_{up}-p_{dn}}{p_{up}}RT - g\ell}\,, \tag{10}$$

where $\ell = \ell_{up} + \ell_{dn}$ is the distance between the upstream and downstream planes, and $\alpha = \ell_{up}/\ell$ is the fraction indicating the location of the orifice between the two pressure sensors.

As long as a well is actively productive, the expression under the last root remains positive. In the field the orifice diameter is adjusted so that the pressure difference is measurable. When little gas is produced, the term $(p_{up} - p_{dn})RT/p_{up}$ diminishes and might become equal to $g\ell$ even with the smallest available orifice, whereat there is no flow and the well is shut off. The accuracy of the flow rate computation is at its best when $g\ell$ is negligible relatively to $(p_{up} - p_{dn})RT/p_{up}$. Therefore most often the term $g\ell$ serves rather to betoken a need to adjust the orifice diameter or deem the well stagnant than an actual correction. Nonetheless, when the chemical activity in the well is slow, yet continuous, the two terms are comparable, whence the term $g\ell$ is imperative in the computation of the mass of gas produced over a long period of time.

There are two important limits to eq. (10): extremely small constriction ratio $\beta \to 0$ and unconstricted pipe $\beta \to 1$. When $\beta \ll 1$, the expression for q_{th} from eq. (10) will read in the denominator $1 - \beta^2 + \mathcal{O}(\beta^4)$, which is asymptotically different from the commonly present factor $\sqrt{1-\beta^4} \sim 1 - \frac{1}{2}\beta^4 + o(\beta^4)$ as in eq. (2), and by comparison not as readily negligible. This amendment accounts for the unconventional location of the pressure sensors and stems from the fact most of the mixing occurs before the jet reaches the downstream pressure sensor, entailing significant losses in the stagnation pressure. This stands in an acute contrast to the common arrangement, where the measurement is taken immediately downstream of the orifice plate. When $\beta = 1$, i.e., the flow faces no occlusion, eq. (10) recovers the Darcy flow (White 1999) corrected for gravity

$$q_{th} = \sqrt{2}\,A_{orf}\sqrt{\frac{D}{\ell f}\left(\frac{p_{up}-p_{dn}}{p_{up}}RT - g\ell\right)} \tag{11}$$

upon defining the friction coefficient as

$$f = 4\left(\alpha c_{f_{up}} + (1-\alpha)c_{f_{dn}}\right). \tag{12}$$

Given that the friction coefficients $c_{f_{up}}$ and $c_{f_{dn}}$ are unknown, it is proposed to make use of these two limits to create a phenomenological model for constriction ratios β that are not extremely small. To this end the notions of a discharge coefficient and an effective friction coefficient are adopted in sections 3.2 and 3.3 respectively. The discharge coefficient is an empirical correction to the flow rate through an orifice, and the friction coefficient is a concomitant attribute of the Darcy flow, also modelled empirically. Both coefficients are known entities and will be adjusted for the current setting to use familiar charts or equations rather than posing an entirely novel empirical model.

Equation (10) can be without loss of generality re-written as

$$q_{th} = \frac{\sqrt{2}\,A_{orf}\,C}{1-\beta^2}\sqrt{\frac{p_{up}-p_{dn}}{p_{up}}RT - g\ell}\,, \tag{13}$$

where C depends on the orifice constriction ratio β, and relative distances between the orifice plate and the pressure tappings ℓ_{up}/D and ℓ_{dn}/D, as is immediately seen from eq. (10). The friction coefficients $c_{f_{up}}$ and $c_{f_{dn}}$ ought be related to the fluid viscosity μ, or in a dimensionless form to the Reynolds number

$$Re = \frac{u\,d\rho}{\mu} = \frac{4\,q\,p}{\pi\,d\mu RT} \tag{14}$$

The coefficient $C(\beta, \ell_{up}/D, \ell_{dn}/D, Re)$ is discussed in detail in section 3.2. Inspired by the form of q_{th} at the limit $\beta = 1$, to wit eq. (11), the adopted form for the flow rate q is

$$q = q_{th}\sqrt{\frac{D}{\ell f_{eff}}} = \frac{\sqrt{2}\,A_{orf}\,C}{1-\beta^2}\sqrt{\frac{D}{\ell f_{eff}}}\sqrt{\frac{p_{up}-p_{dn}}{p_{up}}RT - g\ell} \tag{15}$$

with f_{eff} addressed hereinafter in section 3.3.

The reason for the double multiplicative correction $C\sqrt{\frac{D}{\ell f_{eff}}}$ stems from the twofold physical information stowed in the friction coefficients $c_{f_{up}}$ and $c_{f_{dn}}$. The shear stresses on the walls of the pipe and the ensuing turbulence are affected both by the viscosity of the fluid and the roughness of the surface material. No classic (not empirical) flow equations account for both effects. The discharge coefficient takes into account the Reynolds number, hence addressing the fluid viscosity. The only widely known model dealing directly with the imperfect smoothness of the boundary is Darcy flow (also referred to as Darcy-Weisbach equation) through an empirical equation for the friction coefficient f. On the other hand, Darcy flow is not suited for a contraption containing an orifice, whilst the discharge coefficient was developed precisely for such an arrangement. Here the two were combined into a single empirical model as a way to circumvent the unavailability of the functional dependence of $c_{f_{up}}$ and $c_{f_{dn}}$ on fluid and pipe material properties. It must be remembered that both notions were adopted for this end rather than their primary purport.

3.2. Discharge coefficient

The coefficient $C(\beta, \ell_{up}/D, \ell_{dn}/D, Re)$ can be recognized as the discharge coefficient named after Reader-Harris/Gallagher (or more obsoletely Stolz), an entity well known in the field of flow measurement (ISO 2003), however rarely applied in practice due to the iterative nature of its computation: Re requires the flow rate q for input, then q is re-computed with the found C. In the current setting the procedure was found to converge to a relative error of 10^{-6} in 2–5 iterations. The Reader-Harris/Gallagher equation upon adjustment of notation reads (ISO 2003)

$$C = 0.5961 + 0.0261\beta^2 - 0.216\beta^8 + 0.000521\left(\beta^2\frac{10^6}{Re}\right)^{0.7} + \beta^{3.5}(0.0188 + 0.0063\mathfrak{A})\left(\beta\frac{10^6}{Re}\right)^{0.3} + (0.043 + 0.08\,e^{-10\ell_{up}/D} - 0.123\,e^{-7\ell_{up}/D})(1 - 0.11\mathfrak{A})\frac{\beta^4}{1-\beta^4} - 0.031(\mathfrak{m} - 0.8\mathfrak{m}^{1.1})\beta^{1.3}, \quad \mathfrak{A} = \left(\frac{19000\beta^2}{Re}\right)^{0.8}, \quad \mathfrak{m} = \frac{2\ell_{dn}/D}{1-\beta}. \tag{16}$$

Some comment is in order regarding the dynamic viscosity μ required for the computation of Re. For a gas of k components the dynamic viscosities of the individual components, μ_i, $i = \{1, \ldots, k\}$, vary with temperature according to Sutherland's formula (Crane 1982)

$$\frac{\mu_i}{\mu_{oi}} = \left(\frac{T}{T_{oi}}\right)^{3/2} \frac{T_{oi} + s_i}{T + s_i}, \tag{17}$$

where μ_{oi} and T_{oi} are base viscosity and temperature values respectively, and s_i are corresponding empirical constants.[1] Caution must be exercised in the computation of the kinematic viscosity of a mixture. Here the approach of Davidson (Davidson 1993) was adopted (see also references therein for ad hoc models) as the only one derived based on molecular interaction, to the best of the authors' knowledge. The fluidity of the mixture is obtained via considerations of momentum transfer between colliding molecules, yielding the viscosity as its reciprocal:

$$\mu = \frac{1}{\tilde{f}_{mix}}, \tilde{f}_{mix} = \sum_{i=1}^{k}\sum_{j=1}^{k} \frac{x_i x_j (M_i M_j)^{\frac{1}{2}(a+1)}}{\sqrt{\mu_i \mu_j}\,(M_i + M_j)^a} \Bigg/ \left(\sum_{i=1}^{k} x_i \sqrt{M_i}\right)^2 \tag{18}$$

with $a = 3/8$ being an empirical parameter related to the frequency of collisions (Davidson 1993).

3.3. Turbulence and changes in flow rate

The orifice diameter in the field is adjusted in accord with the production rate of the well. It is not uncommon for the flow rate to attenuate due to a decline in the chemical activity of the well, and an orifice of a smaller diameter must be installed to obtain a measurable pressure drop and an adequate accuracy of the computed flow rate. The Reynolds number in the system is within the interval $0 < Re < 60000$. The turbulence generated in the presence of an occlusion considerably surpasses the expected due to the roughness of the pipe alone. Therefore the setting in question is equivalent to an unobstructed pipe made of a highly abrasive material. It is hence proposed to use this equivalence to determine an effective friction coefficient that will be directly β-dependent.

The classic Darcy-Weisbach flow model combines dimensional analysis and an empirical friction coefficient, based on experimental measurements, to create a realistic flow rate formula, whose purport is to account faithfully for the turbulence engendered by the surface roughness of the conducting pipe (White 1999). This effect cannot be captured by the flow equations that involve properties of the fluid alone, here pressure p, density ρ and viscosity μ. In addition to the Reynolds number computed with the aid of these three quantities, a measure of the roughness of the pipe surface is required. Commonly the surface grain size relatively to the pipe diameter is taken, creating a non-dimensional parameter ε. Then the friction coefficient f in eq. (11) is given by the Colebrook equation (Colebrook 1939; White 1999)

$$\frac{1}{\sqrt{f}} = -2\log_{10}\left(\frac{\varepsilon}{3.7} + \frac{2.51}{Re\sqrt{f}}\right). \tag{19}$$

Equation (19) is implicit in $\sqrt{f}$ and must be solved numerically.[2] It must be noted that eq. (19) corresponds to a fully turbulent flow. The application thereof was deemed justified due to the presence of an abrupt occlusion in the flow that of necessity should initiate turbulence, even if the nominal Re number was below the conventional threshold valid for a simple pipe ($Re \gtrapprox 3000$ in a standard Moody diagram (Moody 1944; White 1999)). Equation (19) is valid over an applicable range of Re numbers, however being phenomenological in essence, does not provide proper limits at $Re \to \infty$ (inviscid limit) and at $Re \to 0$ (stagnation limit).

In the current setting it was desired to have a unique value of ε that captures the global level of turbulence begotten by the constriction. Intuitively, with a higher pressure drop or tighter constriction ratio the turbulence is more pronounced. Hence, as the orifice diameter is always adjusted to the highest possible within the available range $\frac{1}{8} \leqslant \beta \leqslant \frac{1}{3}$, so that the pressure drop is measurable, ε is expected to be identical for all β. Then the friction coefficient is an effective quantity f_{eff} that ought be a function of β. To determine ε and the functional dependence $f_{eff}(\beta)$ a numerical calibration was conducted, whose details are given hereinafter in section 4.

The parameter ε is dimensionless and was found to equal $\varepsilon \approx 0.0367$, valid at least for orifices of constriction ratios $\frac{1}{8} \leqslant \beta \leqslant \frac{1}{3}$ and Reynolds numbers $0 < Re < 60000$. In the classic Darcy-Weisbach flow ε corresponded to the relative roughness of the pipe surface. Here it is an equivalent, global roughness due to the presence of the orifice. Ideally the value of ε ought be verified experimentally, however this is beyond the scope of the current contribution. The given value was based on available experimental data and a sensitivity analysis is presented in section 4.

The function $f_{eff}(\beta)$ was based on the natural compound of Colebrook's eq. (19):

$$\sqrt{f_{eff}} = \sqrt{f}\, k_\beta(\beta) \tag{20}$$

where f is the standard Darcy friction coefficient given by eq. (19), and the function $k_\beta(\beta)$ was established by a numerical calibration based on experimental data with the technical details thereof laid out in section 4. It must be emphasized that the calibration was aimed at a validation of the applicability of Darcy-Weisbach formula with the modification as in eq. (20), and not at a procurement of the most reliable parameter estimate.

4. Comparison to quondam model

The model implemented to compute the flow rate heretofore was based on a variant of the classic flow meter model (eq. 2) corrected for gravity

$$q_{exp} = C_{exp} A_{orf} \sqrt{\frac{p_{up} - p_{dn}}{p_{up}} RT - g\ell} \tag{21}$$

where C_{exp} is a constant, obtained experimentally through the calibration of the flowmeter for a flow of air at standard conditions of 20 °C and 1 atm with the pressure sensors installed at the distances of $2D$ upstream and downstream of the orifice plate. The coefficient C_{exp} differed from the calibration constant provided by the flowmeter manufacturer because of the unconventional sensor locations and had been initially calibrated to yield a better accuracy with higher flow rates, as the wells with a greater pro-

[1] An exponential law (White 1999) $\frac{\mu_i}{\mu_{oi}} = \left(\frac{T}{T_{oi}}\right)^{n_i}$ might also be used with n_i being a set of empirical constants instead of s_i.

[2] There are several iterative schemes of excellent convergence, e.g., Serghides's solution based on Steffensen's method to find roots of transcendental equations numerically. The solutions are also graphed on Moody diagram, however that is inconvenient to be used in frequent computations.

Fig. 2. Least squares fit in the calibration of the parameters m and n. The four diamond denoted points correspond to β = 1/3, 1/4, 1/6, 1/8.

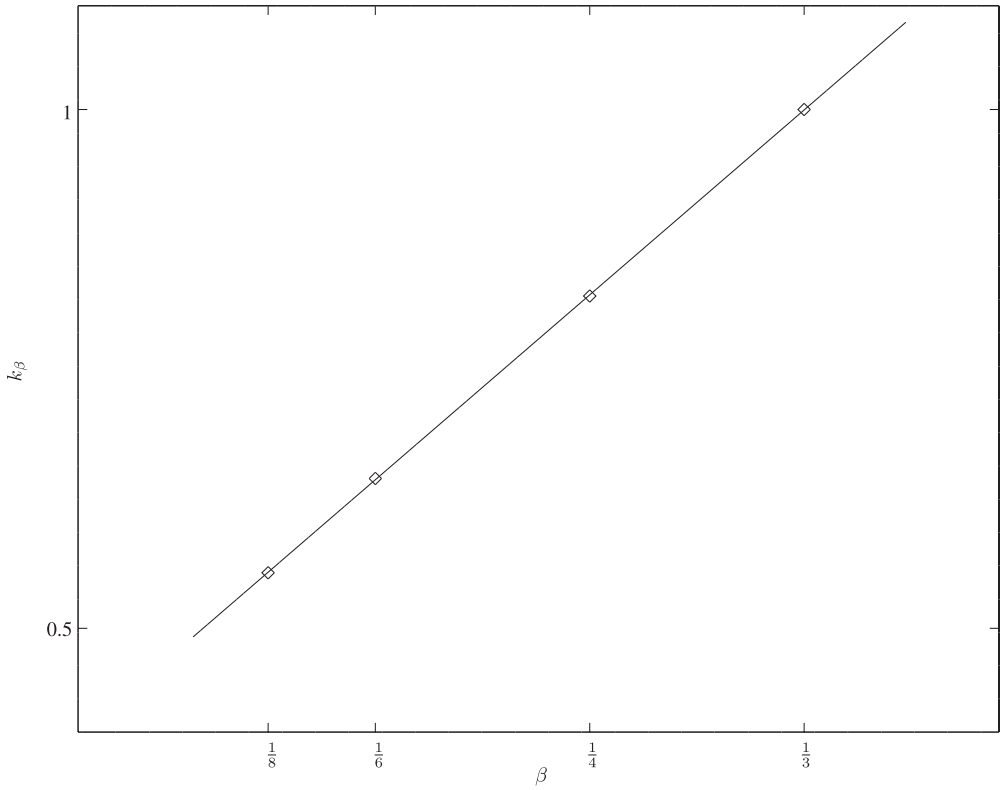

duction contributed the predominant mass of gas. The flow rate q_{exp} was corrected for atmospheric conditions and gas mixture as in section 2. Hence eq. (21) gave reliable results as long as the measurements fell in a close vicinity of the calibration point.

The purpose of the numerical calibration is twofold. First is to determine such value for ε and functional form $k_\beta(\beta)$ that the proposed model recovers the results obtained with eq. (21) for a set of reliable measurements and furthermore affords sufficient flexibility to account for variation in β, when the well activity fluctuates. This part is referred to as calibration. Second is to verify that with these optimal settings the results of the two models match reasonably based on a broad collection of measurements, comprising validation thereof.

4.1. Numerical calibration

The function $k_\beta(\beta)$ was sought as a power series, and it was established that a linear approximation

$$k_\beta(\beta) = m\beta + n + o(\beta) \tag{22}$$

sufficed to capture the variation of friction coefficient with β faithfully.[3] To obtain optimal values for ε, m, and n the flow rate as computed with the model described in section 3 is to be compared to the rate computed with eq. (21), the model employed hitherto. To this end a small set of reliable measurements was taken and the parameters ε, m and n were adjusted by minimization of the error $\epsilon = |q/q_{\text{exp}} - 1|$, with q and q_{exp} given by eq. (15) and eq. (21) respectively. A set of 20 recordings of the format

Table 1. Model validation: mean $\bar{\epsilon}$ and standard deviation s of the absolute error $\epsilon = |q/q_{\text{exp}} - 1|$ for a sample of wells with various orifice constriction ratios.

	$\beta = \frac{1}{3}$	$\beta = \frac{1}{4}$	$\beta = \frac{1}{6}$	$\beta = \frac{1}{8}$	all
Number of wells	440	115	95	150	800
$\bar{\epsilon}$ (%)	0.45	0.9	1.1	2.5	1.0
s (%)	0.96	1.1	1.1	3.8	2.0

Note: Flow rates q and q_{exp} are computed with eq. (15) and eq. (21) respectively. Overall instrumental measurement error is approximately 5%.

$$\{p_{\text{up}},\ p_{\text{dn}},\ T,\ x_{CH_4},\ x_{O_2},\ x_{CO_2}\}$$

was used. The fractions x_{CH_4}, x_{O_2}, x_{CO_2} are necessary to compute the gas constant R and viscosity μ according to eq. (5) and eq. (18), to be used with p_{up}, p_{dn} and T to obtain the flow rate. Out of the 20 recordings 11 were for β = 1/3, utilized to obtain an optimal value of ε alone.[4] The remaining 9 recordings were for β = 1/4, 1/6, 1/8 (3 recordings for each value of β), and k_β was varied iteratively to minimize the error ϵ with ε fixed at its optimal value. The dimensionless coefficients m and n were then determined by a least squares fit and found to equal $m \approx 2.2$, $n \approx 0.3$. Figure 2 depicts the linear regression.

The choice of recordings for the calibration was guided saliently by a significant measured pressure drop, since C_{exp} in the quondam model (eq. 21) had been chosen for the best accuracy in that work regime. Inclusion of more recordings in the numerical cali-

[3]It is conjectured that for values of β closer to unity higher order terms might become indispensable.

[4]Without loss of generality $k_\beta = 1$ for $\beta = 1/3$, as a different choice of $k_\beta(1/3)$ would have yielded somewhat different values of ε, m, n and shifted the regression line. This is possible since ε is a virtual roughness and not an immediate physical parameter.

Fig. 3. (*a*) Upper and lower bounds of δq, the variation of flow rate q with the equivalent roughness ε. The point of intersection of both curves is the nominal optimum $\varepsilon = 0.0367$, serving as the reference point for the computation of % change. In absolute value the upper bound corresponds to $|\Delta p| \gg 1$ and the lower bound – to $|\Delta p| \to 0$. (*b*) Blow up of the region near the intersection point. Note that δq is virtually linear in ε and the maximal $|\delta q|$ does not exceed the overall instrumental measurement error of approximately 5%.

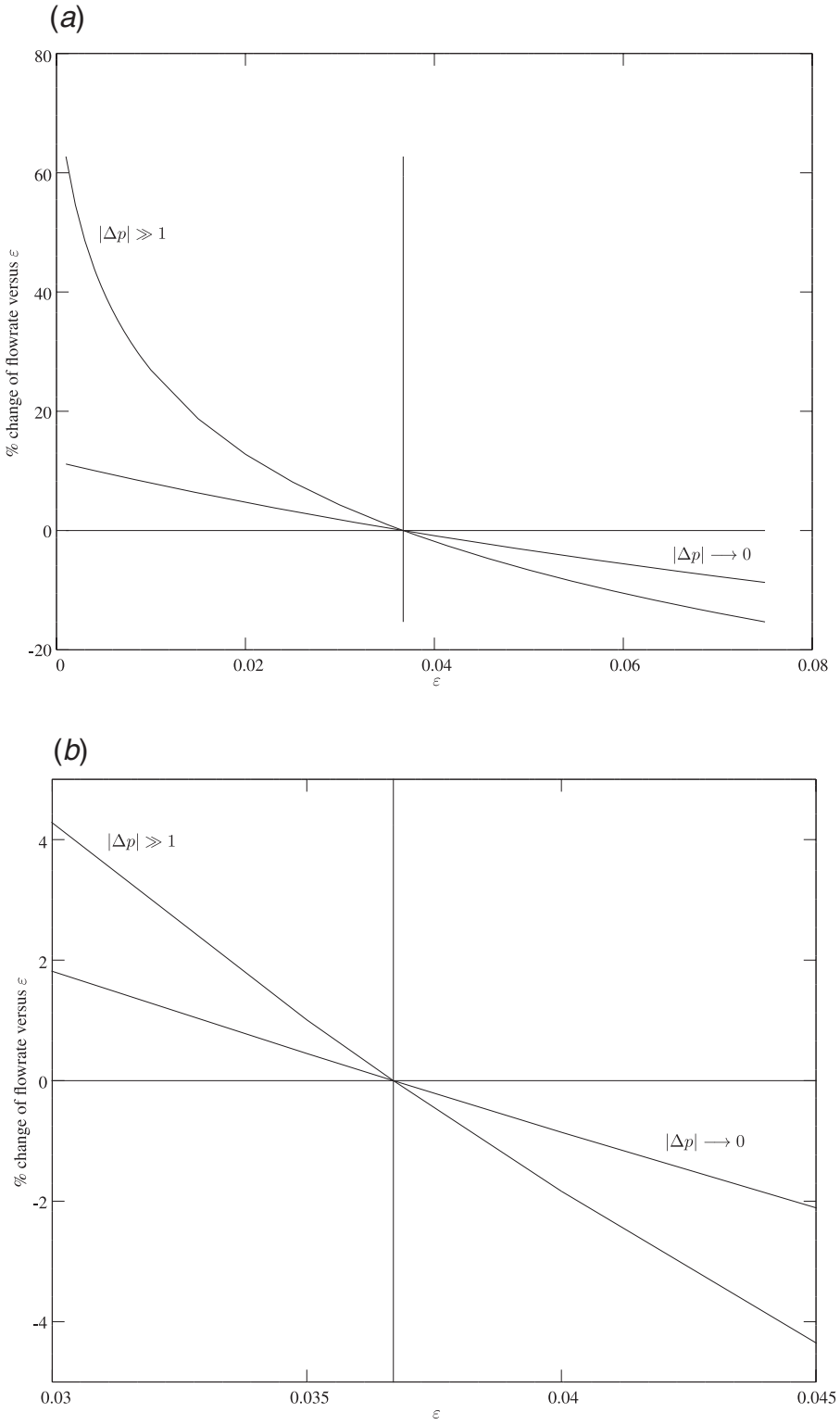

bration affected the higher decimal places in the values of ε, m and n without yielding convergence, wherefore seeking a higher precision for these parameters is incongruent with the instrumental measurement error.

4.2. Validation

The entire model was thereupon validated through the computation of flow rates for 800 recordings (distinct from the ones used in the calibration). The results are summarized in Table 1. It is seen

that for all orifice sizes in question the two models match well for the higher orifice sizes. As expected, the fit somewhat deteriorates at the smallest orifice, where the flow is often slow and the measurements not as accurate.

The sensitivity of q to variations in ε was tested for different (fixed) values of the pressure drop $|\Delta p| = p_{up} - p_{dn}$. Figure 3 depicts the lower and upper bounds of the change δq about the nominal point $\varepsilon = 0.0367$ for the lowest and highest flow rates from the set of 800 recordings. Within the two bounds the variation δq is highly non-linear in response to changes in $|\Delta p|$ for a fixed ε: for instance, a curve for 1/3 of the pressure drop corresponding to the upper bound would have been virtually indistinguishable therefrom. The variation δq for a fixed $|\Delta p|$ is obviously non-linear in ε. In reality ε is expected to deviate but slightly from the optimal point $\varepsilon \approx 0.0367$, whereat δq is virtually linear in ε and the maximal $|\delta q|$ does not exceed the overall instrumental measurement error of approximately 5%.

5. Discussion

The presented model combined several developments in the field of fluid dynamics in conjunction with a number of unique modifications to conform to the unordinary geometry of the setting. A small sample of recordings was used for a numerical calibration of a set of dimensionless parameters. The model was thereafter validated with a large sample of recordings. Out of the four orifice sizes tested, the fit quality is good for $\beta = 1/4, 1/6$, slightly better for $\beta = 1/3$, somewhat worse for $\beta = 1/8$, and deep within the measurement error bounds for all β in the range.

The fit is better for larger constriction ratios because C_{exp}, the sole parameter of the quondam model (eq. 21), was calibrated for relatively high flow rates to suit the practical ends, maximizing the accuracy of the computed mass of gas produced annually. To paraphrase, eq. (21) entailed no flexibility to account for the significant variation in the measured pressure drop, when the chemical processes within an active landfill followed their natural, yet absolutely uncontrollable course. An optimal value of C_{exp} was a pragmatic, crude approach to account for the various phenomena affecting the flow in a well. A constant C_{exp} is equivalent to an utter disregard of the dependence of $C(\beta, \ell_{up}/D, \ell_{dn}/D, Re)$ on its four arguments. In particular, continuously changing reaction rates within the landfill impacting both the amount and composition of the produced gas, with the ensuing changes in flow rate, fluid viscosity and gas constant, are responsible for changes in the Reynolds number. Variation of the Reynolds number with the ambient temperature appears less significant, however its cumulative influence over an annual cycle is not to be dismissed. The new model takes into consideration the varying therefore Reynolds number and further uses it as input to account for the turbulence engendered by the presence of the orifice. The global equivalent roughness of the setting is given by ε, a parameter uniform for all constriction ratios β in question, and the dependence of the effective friction coefficient f_{eff} on β is modelled via a markedly linear relationship.

The proposed model is serviceable in the computation of the gas flow rate in any similar setting and is modular, permitting adjustment and use of its three parts as necessary. Possible modifications are listed below.

Regarding the theoretical flow rate, if, for instance, the pressure tappings are placed conventionally, the factor $1 - \beta^2$ in eq. (13) can be replaced by $\sqrt{1 - \beta^4}$ (or neglected by setting $\beta = 0$) and the pressure difference $p_{up} - p_{orf}$ used for input.

It is believed that the discharge coefficient as computed by Reader-Harris/Gallagher equation results in a better accuracy than a unique constant. With the computational resources available today the implementation of eq. (16) is not overly burdensome. Nonetheless at will the discharge coefficient can be taken as the leading order term in eq. (16) or equivalently setting $\beta = 0$ therein.

If the turbulence part is not used, the computed flow rate is likely to be underestimated. To implement this correction one will require a onetime access to a set of independent measurements of good precision and consistence. If a unique constriction ratio is used, an optimal value for the equivalent roughness parameter ε can be obtained as described in section 4. If the orifice aperture is adjustable, the slope m and intercept n of k_β ought be found by error minimization and then regression.

If all three parts are combined, the resulting flow rate is based on momentum and mass conservation as given by the equations for an incompressible fluid, corrected empirically for non-uniformity and viscosity.

Acknowledgement

The authors acknowledge the financial support of the National Research Council IRAP program, contribution agreement #829583. Y.N. is thereby beholden to Prof. G. Iosilevskii (Technion, IIT) for meaningful discussions.

References

Batchelor, G.K. 1990. Introduction to fluid dynamics. Cambridge.

Colebrook, C.F. 1939. Turbulent flow in pipes, with particular reference to the transition region between the smooth and rough pipe laws. Journal of the Institution of Civil Engineers, **11**: 133–156. doi:10.1680/ijoti.1939.13150.

Crane, Co. 1982. Flow of fluids through valves, fittings and pipe. Technical paper No. 410M, 300 Park Avenue, New York, NY 10022, appendix A-5.

Davidson, T.A. 1993. A simple and accurate method for calculating viscosity of gaseous mixtures. Report of investigations, US Department of the Interior, Bureau of Mines.

ISO. 2003. Measurement of fluid flow by means of pressure differential devices inserted in circular cross-section conduits running full - part 2: Orifice plates. European Committee for Standardization, EN ISO 5167-2:2003 E, pp. 11–12.

Moody, L.F. 1944. Friction factors for pipe flow. Transactions of ASME, **66**: 671–684.

White, F.M. 1999. Fluid mechanics. McGraw Hill 4th edition.